Probability distribution of hard-disk and hard-sphere gases over finite subvolumes

F. L. Román, J. A. White, and S. Velasco
Departamento de Física Aplicada, Facultad de Ciencias, Universidad de Salamanca, 37008 Salamanca, Spain
(Received 2 May 1995; revised manuscript received 12 July 1995)

The probability distribution of a gas consisting of N_0 hard disks (hard spheres) over finite subvolumes is modeled by the hypergeometric distribution. The effects of mutual exclusion between particles are incorporated by a density dependent effective volume per particle. This effective volume is related to the fluctuation in particle number. The behavior of the computed effective volume is compared with analytical expressions calculated from well-known equations of state. Corrections for this effective volume due to the considered finite-size effects are proposed.

PACS number(s): 61.20.Gy, 05.50.+q, 64.60.Kw

The problem of calculating the probability distribution of atoms or molecules over finite subvolumes can be of interest for modeling a number of problems arising in biology, chemistry, and physics. Applications include phenomena associated with adsorption on solid surfaces, configuration of fluid structures, condensation or coagulation problems, or the distribution of guest molecules over zeolite cavities.

For an ideal gas, composed of N_0 interactionless point particles enclosed in a volume V_0, the probability of finding N particles in a subvolume V is given by the binomial distribution

$$W(N) = \binom{N_0}{N} p^N (1-p)^{N_0-N} \tag{1}$$

with $p = V/V_0$. However, real molecules have finite size which leads to the fact that the probability of large values of N is reduced. On the basis of the statistical problem of sampling without replacement, Güémez and Velasco [1,2] showed that the distribution of finite size particles among mutually exclusive lattice sites (lattice gas model) is given by the hypergeometric distribution

$$W(N) = \frac{\binom{N_0}{N}\binom{M-N_0}{K-N}}{\binom{M}{K}}, \tag{2}$$

where M and K are the number of lattice sites available in V_0 and V, respectively, being $K/M = V/V_0$.

Besides its intrinsic interest, an advantage of using the hypergeometric distribution (2) is that it gives explicit expressions for the mean particle number,

$$\langle N \rangle = N_0 \frac{K}{M} = N_0 \frac{V}{V_0} \tag{3}$$

and for the dispersion,

$$\Delta^2(N) = N_0 \frac{K}{M}\left(\frac{M-K}{M-1}\right)\left(1-\frac{N_0}{M}\right) = N_0 \frac{V}{V_0}\frac{\left(1-\frac{V}{V_0}\right)}{\left(1-\frac{1}{M}\right)}\left(1-\frac{N_0}{M}\right) \tag{4}$$

in terms of the parameters characterizing the problem. A crucial point in order to apply the hypergeometric function to model specific systems is that dispersion (4) depends on the number M of lattice sites available in the total volume V_0, for which an upper bound is corresponding to close packing. In particular, with this choice, Rowlinson and Woods [3] have compared the hypergeometric distribution with computer simulations of the distribution of methane molecules in NaY zeolite cavities, showing that simulated distributions are narrower than hypergeometric predictions. In general this is an expected result since distribution (2) refers to a gas for which particles are not free to occupy any point in space, while in real fluids the particles move continuously and they present a less-accommodating configuration for placement in an arbitrary subvolume than for the close-packing case. This leads to an effective value of the number M lower than that corresponding to close-packing and, in accordance with Eq. (4), to a decrease in the dispersion of the hypergeometric distribution.

The hypergeometric distribution has also been used by Chmelka *et al.* [4] to describe the experimental distribution of Xe atoms in NaA zeolite cavities. These authors use the hypergeometric distribution with the mean occupancy number $\langle N \rangle$, and the quantities K and V/V_0 provided by the best fits to the data over the range of Xe occupancies investigated by changing the Xe loading, but with a fixed value of M for all the reported fits. In the cases examined by these authors, agreement is excellent between the hypergeometric fits and those obtained experimentally, except at the highest Xe loading, for which the observed Xe distribution is also narrower than the hypergeometric prediction.

The concrete application of the hypergeometric function to model the statistical distribution of particles in zeolite cavities shows clearly the importance of exclusion particle effects on the fluid behavior. In this work, we propose to describe these exclusion effects by means of a density (ρ) dependent excluded volume per particle, $\nu = \nu(\rho)$, so that $M = V_0/\nu(\rho)$. Then, Eq. (4) allows one to relate exclusion effects with fluctuations in particle number. Since, at least in the thermodynamic limit, these fluctuations can be derived from the compressibility factor, we have a simple way to connect exclusion effects

with equilibrium properties of the fluid.

We shall proceed as follows. First, we analyze the statistical distribution of hard D spheres ($D = 2$ and 3) over finite subvolumes by means of Monte Carlo (MC) simulations. Second, the obtained distributions are described by the hypergeometric function (2) with the same dispersion that the simulated distribution. Finally, an effective (excluded) volume per particle, $\nu = \nu(\rho)$, is computed from Eq. (4) with $M = V_0/\nu(\rho)$.

The simulations were done using standard MC techniques for N_0 hard particles in square or cubic boxes of side L_0 ($V_0 = L_0^D$) with periodic boundary conditions. The subvolume V (of side L) was located at the center of the box with sides parallel to those of V_0. The number N of particles into the subvolume V was calculated as the number of hard D spheres whose center was located in the subvolume. The number density is $\rho = N_0/V_0$ and η the corresponding packing fraction, which is defined by

$$\eta = \frac{\pi^{D/2} R^D}{\Gamma(1 + \frac{D}{2})} \rho, \tag{5}$$

where $\Gamma(x) =$ is the gamma function and R the real radius. Furthermore, since well-established hard-disk and hard-sphere fluid-solid transitions occur to high enough values of the packing fraction, we have done the MC simulations for $\eta < 0.65$ for the hard-disk case and for $\eta < 0.45$ for the hard-sphere case, i.e., below the fluid coexistence density in both cases ($\eta \approx 0.690$ for $D = 2$, $\eta \approx 0.494$ for $D = 3$). The simulations were done on square boxes of sides $L/R = 13$ to 89, and on cubic boxes of sides $L/R = 11$ to 37. The subvolume size was taken $V = V_0/4$.

Figures 1 and 2 show two typical distributions obtained by computer simulation on a cubic box of side $L/R = 12.5$ and $N_0 = 64$ ($\eta = 0.10$) and a cubic box of side $L/R = 12.5$ and $N_0 = 144$ ($\eta = 0.31$). For these cases, the dispersions associated with the simulated distributions are $\Delta^2(N) = 5.554$ and $\Delta^2(N) = 6.982$, respectively. These distributions are then modeled by the binomial form (1), the hypergeometric form (2) with M given by the number of lattice sites inside the box corresponding to a hexagonal close packing (HCP) lattice ($M = 345$ in both cases), and the hypergeometric form (2) with M obtained from Eq. (4) and by using the dispersions of the computed distributions ($M = 117.98$ and $M = 191.84$, respectively). These theoretical distributions are also plotted in Figs. 1 and 2, where the differences between the observed distributions and the modeled ones are also shown. It is clear that the observed distributions are much narrower than the binomial, considerably narrower than the hypergeometric with M given by the HCP lattice, and in excellent agreement with the hypergeometric with the dispersion given by the simulated distributions.

The effective volume per particle is obtained from Eq. (4) with $\nu = V_0/M$,

$$\nu(\eta; L_0) = \frac{N_0 \frac{V}{V_0}\left(1 - \frac{V}{V_0}\right) - \Delta^2(N; L_0)}{N_0^2 \frac{V}{V_0}\left(1 - \frac{V}{V_0}\right) - \Delta^2(N; L_0)} V_0 \tag{6}$$

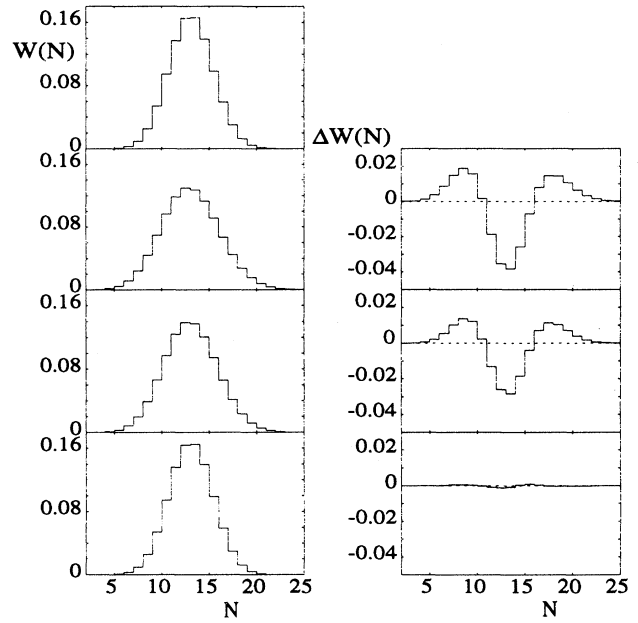

FIG. 1. The distribution of hard spheres for $L_0/R = 12.5$ and $N_0 = 64$ over a subvolume $V = V_0/4$ ($V_0 = L_0^3$). The left-hand column shows, from the top, the distribution observed by MC simulation and the binomial, the hypergeometric with a HCP lattice, and the hypergeometric with dispersion equal to the observed distribution. The right-hand column shows the differences between the three model distributions and the observed one.

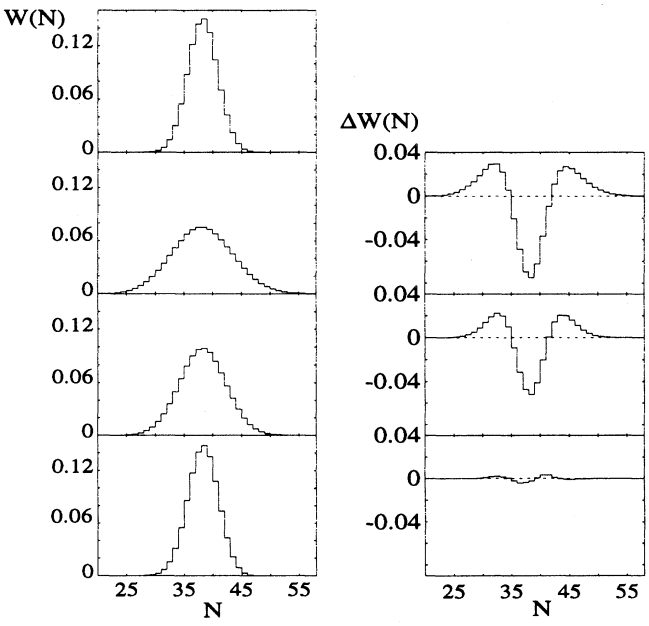

FIG. 2. Same caption as Fig. 1 but for $L_0/R = 12.5$ and $N_0 = 144$.

and with the dispersion $\Delta^2(N;L_0)$ given by the computed distribution. The variation of the effective volume per particle versus the packing fraction for various boxes sizes is shown in Fig. 3(a) for the hard-disk case and in Fig. 3(b) for the hard-sphere case. These results confirm our expectations: as the packing fraction (density) decreases, the effective volume per particle increases. Moreover, these results also show that for a fixed value of η the effective volume per particle increases with the box size, approaching a limiting value.

Furthermore, the dependence of the above results on the subvolume size is also of interest. In Fig. 4 we have plotted the effective volume per particle ν versus the ratio L/R for $L_0/R = 45$ and for two intermediate packing fractions ($\eta = 0.403$ for $D = 2$ and $\eta = 0.170$ for $D = 3$). We have found that ν remains practically invariant in a range of subvolume sizes such that $6 \leq L/R \leq 41$ for $D = 2$, while this range is more reduced, $12 \leq L/R \leq 39$, for $D = 3$. This behavior does not change appreciably with the packing fraction. This fact means that the subvolume size must be chosen large enough so that edge effects can be neglected. Also one should avoid edge effects in the remaining subvolume $(V_0 - V)$, and restrict the maximum subvolume size accordingly.

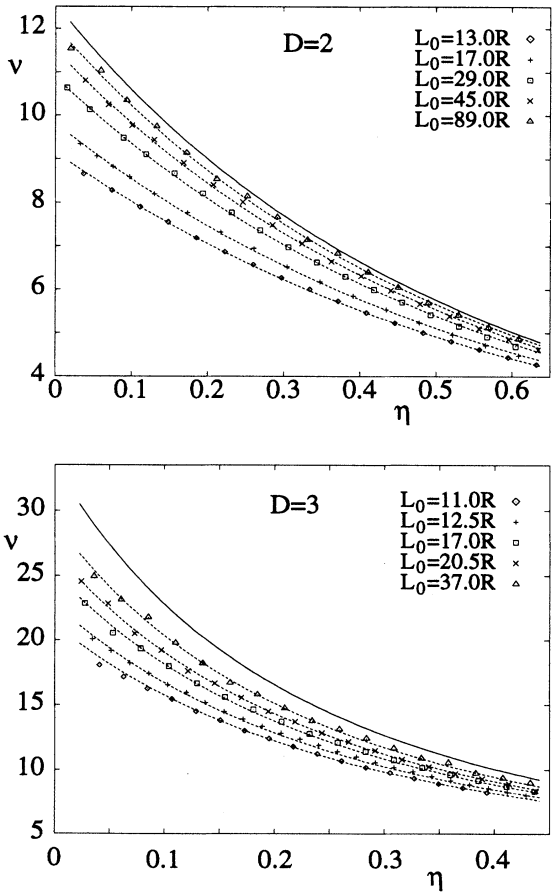

FIG. 3. Behavior of the effective excluded volume per particle ν versus the packing fraction η for hard disks ($D = 2$) and hard spheres ($D = 3$), and for different sizes of the box side L_0. Symbols stand for ν obtained from Eq. (6) with dispersion $\Delta^2(N;L_0)$ given by the computed distribution. Solid lines stand for Eq. (11) with $b = 0$ ($D = 2$) and for Eq. (13) with $b = 0$ ($D = 3$). Dashed lines correspond to ν obtained from Eqs. (21) and (22), and parameters ξ_2 and ξ_3 given in Fig. 7.

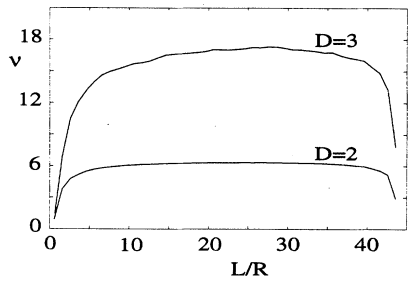

FIG. 4. Dependence of the effective volume per particle ν with the ratio L/R for $L_0 = 45R$ and for $\eta = 0.403$ ($D = 2$) and $\eta = 0.170$ ($D = 3$).

In the thermodynamic limit, Eq. (6) becomes

$$\nu(\eta) = \frac{\pi^{D/2}R^D}{\Gamma(1+\frac{D}{2})}\frac{1}{\eta}\left[1 - \frac{\Delta^2(N)}{\langle N\rangle}\right] \tag{7}$$

with the mean value $\langle N\rangle$ given by Eq. (3) and where we have used the notation $\nu(\eta) \equiv \nu(\eta;\infty)$ and $\Delta^2(N) \equiv \Delta^2(N;\infty)$. On the other hand, from the compressibility factor, $Z(\eta)$, we can derive the relative fluctuation as [5]

$$\frac{\Delta^2(N)}{\langle N\rangle} = k_B T \rho \chi_T = \left[\frac{\partial}{\partial\eta}[\eta Z(\eta)]\right]^{-1}, \tag{8}$$

where χ_T is the isothermal compressibility and T the absolute temperature. From Eqs. (7) and (8) one gets

$$\nu(\eta) = \frac{\pi^{D/2}R^D}{\Gamma(1+\frac{D}{2})}\frac{1}{\eta}\left\{1 - \left[\frac{\partial}{\partial\eta}[\eta Z(\eta)]\right]^{-1}\right\} \tag{9}$$

which provides the basis for deriving the excluded volume $\nu(\eta)$ from the compressibility $Z(\eta)$.

For the hard-disk case ($D = 2$) the simplest equations of state are of the type

$$Z(\eta) = \frac{1 + b\eta^2}{(1-\eta)^2} \tag{10}$$

which contains the results of the scaled particle theory (SPT) ($b = 0$) [6] and the Henderson (H) equation of state ($b = 0.125$) [7]. Using Eqs. (9) and (10), one gets

$$\nu(\eta) = \pi R^2\left[\frac{4 - 3(1-b)\eta + (1-b)\eta^2}{1 + \eta + 3b\eta^2 - b\eta^3}\right] \quad (D = 2). \tag{11}$$

For the hard-sphere case ($D = 3$) the simplest expressions for $Z(\eta)$ have the form [5]

$$Z(\eta) = \frac{1 + \eta + \eta^2 - b\eta^3}{(1-\eta)^3} \tag{12}$$

which contains the results of the Percus-Yevick compressibility (PY-c) ($b = 0$) and the Percus-Yevick virial (PY-v) ($b = 3$) equations, as well as the Carnahan-Starling (CS) equation ($b = 1$). Using Eqs. (9) and (12), one gets

$$\nu(\eta) = \frac{4}{3}\pi R^3 \left[\frac{(4-\eta)[2+(1-b)\eta^2]}{1+4\eta+4\eta^2-4b\eta^3+b\eta^4}\right] \quad (D=3). \tag{13}$$

We note that the all reported analytical expressions for $\nu(\eta)$ verify the conditions $\nu(0) = \pi^{D/2}(2R)^D/\Gamma(1+\frac{D}{2})$ and $\nu(1) = \pi^{D/2}R^D/\Gamma(1+\frac{D}{2})$. Furthermore, we found that $\nu(\eta)$ shows very little sensitivity to $Z(\eta)$. In particular, the effective volume per particle $\nu(\eta)$ given by Eq. (11) with $b = 0$ (SPT) for hard disks and by Eq. (13) with $b = 0$ (PY-c) for hard spheres is plotted with solid lines in Figs. 3(a) and 3(b), respectively.

On the other hand, some expressions for the direct correlation function (DCF) of a hard-core fluid have been recently proposed on a semiempirical basis [8,9]. The proposal is based on the geometrical concept of the overlap volume of two D spheres with an effective (rescaled) radius $R' = a\,R$, the scaling ratio a being a density dependent quantity, i.e., $a = a(\eta)$. In the present context $\nu(\eta)$ and $a(\eta)$ are related by

$$\nu(\eta) = \frac{\pi^{D/2}R'^D}{\Gamma(1+\frac{D}{2})} = \frac{\pi^{D/2}R^D}{\Gamma(1+\frac{D}{2})}a(\eta)^D. \tag{14}$$

Then, Eq. (9) leads to

$$a^D = \frac{1}{\eta}\left\{1-\left[\frac{\partial}{\partial\eta}[\eta Z(\eta)]\right]^{-1}\right\}, \tag{15}$$

i.e., our hypergeometric model provides a simple expression for determining the scaling parameter $a(\eta)$ in terms of a prescribed equation of state. Baus and Colot (BC) [8] have found a different equation for determining $a(\eta)$ in terms of $Z(\eta)$ by imposing in the obtained DCF the same degree of thermodynamic consistency as in the Percus-Yevick DCF.

To test Eq. (15) (and thus the hypergeometric model) we can compare with BC results. No analytical results are known for hard disks ($D = 2$) in the BC approach. In this case, by fitting numerical results, Baus and Colot [9] give the expression

$$a_{\rm BC}(\eta) = \frac{2+\eta\alpha(\eta)}{1+\eta+\eta\alpha(\eta)} \quad (D=2) \tag{16}$$

with $\alpha(\eta) = -0.2836 + 0.2733\eta$.

In our framework, from Eqs. (10) and (15) [or, equivalently, from Eqs. (11) and (14)] one gets

$$a_{\rm SPT}(\eta) = \left[\frac{4-3\eta+\eta^2}{1+\eta}\right]^{\frac{1}{2}}, \tag{17}$$

$$a_{\rm H}(\eta) = \left[\frac{32-21\eta+7\eta^2}{8+8\eta+3\eta^2-\eta^3}\right]^{\frac{1}{2}}. \tag{18}$$

These equations are compared with $a_{\rm BC}(\eta)$ given by Eq. (16) in Fig. 5. We can see discrepancies smaller than a 0.5% between our results and BC results.

In the case of hard spheres ($D = 3$), using the PY-c equation of state, Baus and Colot [9] have obtained

$$a_{\rm BC}(\eta) = \frac{2+\eta}{1+2\eta} \quad (D=3). \tag{19}$$

From Eqs. (12) and (15) with $b = 0$ [or, equivalently, from Eqs. (13) and (14)] one gets

$$a_{\rm PY-c}(\eta) = \left[\frac{(4-\eta)(2+\eta^2)}{(1+2\eta)^2}\right]^{\frac{1}{3}}. \tag{20}$$

This equation is compared with $a_{\rm BC}(\eta)$ given by Eq. (19) in Fig. 6. We can also see discrepancies smaller than 0.6% between our results and BC results.

Finally, we analyze the problem of the influence of the size of the system on the excluded volume. Figure 3 shows clearly the results for $\nu(\eta; L_0)$ obtained by modeling the MC simulations with the hypergeometric distribution approach to the limiting analytical results as L_0 increases. Since we have found that there are no significative differences between the results for the excluded volume obtained from different equations of state, we shall study finite size effects on only the SPT case for hard disks and the PY-c case for hard spheres (recall that PY-c coincides with SPT for $D = 3$). In order to take into account these finite size effects we propose to modify Eqs. (16) and (19) with $b = 0$ in the form

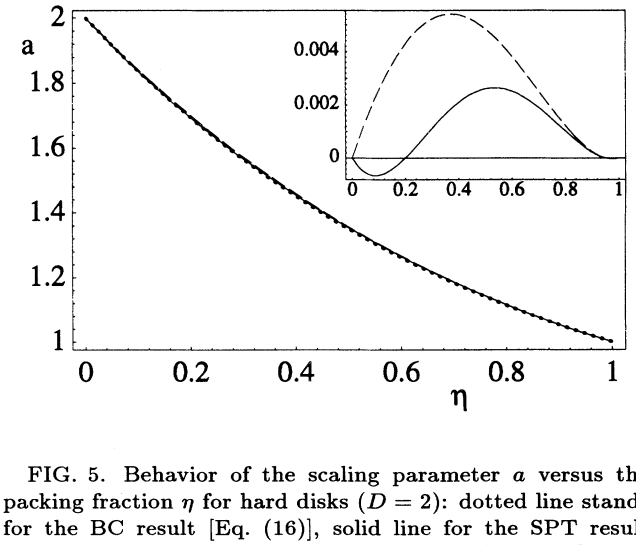

FIG. 5. Behavior of the scaling parameter a versus the packing fraction η for hard disks ($D = 2$): dotted line stands for the BC result [Eq. (16)], solid line for the SPT result [Eq. (17)], and dashed line for the H result [Eq. (18)]. The inset shows the relative differences $(a_{\rm SPT} - a_{\rm BC})/a_{\rm BC}$ (solid line) and $(a_{\rm H} - a_{\rm BC})/a_{\rm BC}$ (dashed line) versus η.

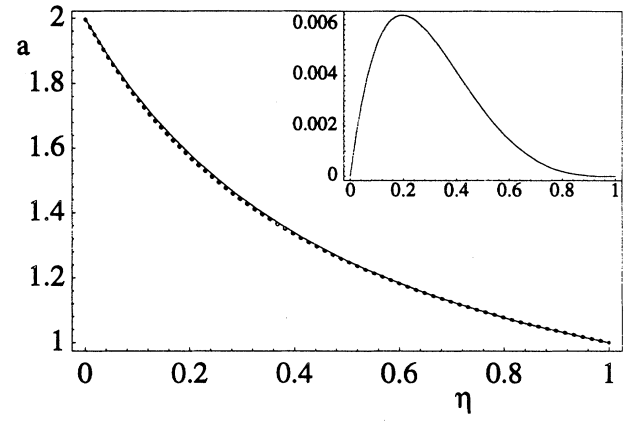

FIG. 6. Behavior of the scaling parameter a versus the packing fraction η for hard spheres ($D = 3$): dotted line stands for the BC result [Eq. (19)] and solid line for the PY-c result [Eq. (20)]. The inset shows the relative difference $(a_{\mathrm{PY-c}} - a_{\mathrm{BC}})/a_{\mathrm{BC}}$ versus η.

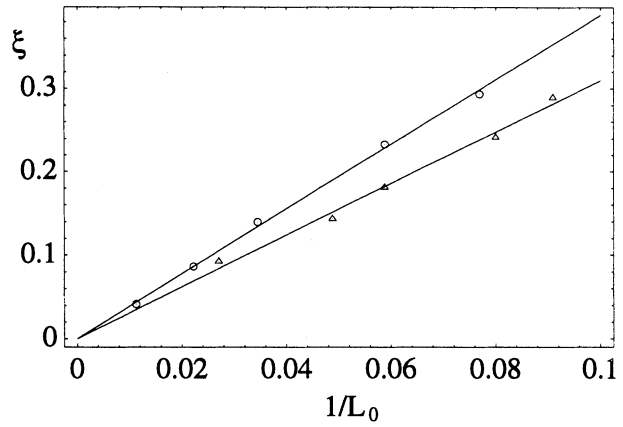

FIG. 7. Behavior of the parameters ξ_2 (○) and ξ_3 (△) [see Eqs. (21) and (22)] versus the inverse of the box side R/L_0. Solid lines stand for the corresponding least-squares fit.

$$\nu_{\mathrm{SPT}}(\eta;\xi_2) = \pi R^2 \left[\frac{(2-\xi_2)^2 - (3-2\xi_2)\eta + \eta^2}{1+(1-\xi_2)^2\eta}\right] \quad (D=2), \tag{21}$$

$$\nu_{\mathrm{PY-c}}(\eta;\xi_3) = \frac{4}{3}\pi R^3 \left[\frac{(2-\xi_3)^3 - (2-\xi_3)\eta + (2-\xi_3)^2\eta^2 - (1-\xi_3)^3\eta^3}{[1+2(1-\xi_3)\eta]^2}\right] \quad (D=3), \tag{22}$$

where the parameters ξ_2 and ξ_3 depend on the size of the system and are determined from a nonlinear fit of Eqs. (21) and (22) with $\nu(\eta; L_0)$ obtained from the MC simulations data. These fits are shown in Figs. 3(a) and 3(b) with dashed lines. The corresponding values of ξ_2 and ξ_3 versus R/L_0 are plotted in Fig. 7 and we see an excellent straight-line behavior in both cases. A least-squares fit yields $\xi_2 = (3.88 \pm 0.13)R/L_0$ and $\xi_3 = (3.10 \pm 0.17)R/L_0$.

We have also analyzed the finite size effects on the BC results for the scaling parameter $a(\eta)$. We propose to modify Eqs. (16) and (19) in the form

$$a_{\mathrm{BC}}(\eta,\xi_2) = \frac{2-\xi_2+\eta\alpha(\eta)}{1+(1-\xi_2)\eta[1+\alpha(\eta)]} \quad (D=2), \tag{23}$$

$$a_{\mathrm{BC}}(\eta,\xi_3) = \frac{2-\xi_3+\eta}{1+(2-\xi_3)\eta} \quad (D=3), \tag{24}$$

with the values $\xi_2 = (3.86 \pm 0.18)R/L_0$ and $\xi_3 = (3.10 \pm 0.24)R/L_0$.

At this point it must be noticed that Eqs. (21)–(24) are simple modifications of the expressions in the thermodynamic limit. These modifications have been proposed heuristically in order to reproduce the MC results and without a microscopic basis. The reason for this procedure is twofold: first, by analyzing the values taken by the parameters ξ_2 and ξ_3 one can easily establish a finite size behavior in the MC data, and second, it is not clear (if possible) how to obtain and approximate expression for $\nu(\eta)$ [or $a(\eta)$] in a finite system because we lack a well defined equation of state and, furthermore, the expression (8) linking fluctuations with the equation of state will certainly not hold.

To conclude, we have shown that the statistical distribution of hard disk and hard sphere fluids in finite subvolumes can be described by a hypergeometric distribution by incorporating a density dependent effective (excluded) volume per particle ν. From this idea, this study connects the exclusion effect between particles with the fluctuations in the particle number, and so with the equation of state. The problem of the influence of the size system on the excluded volume has been also addressed.

ACKNOWLEDGMENTS

This work was supported by the Dirección General de Investigación Científica y Técnica (DGICYT) of Spain under Grant No. PB 92-0279.

[1] J. Güémez and S. Velasco, Am. J. Phys. **55**, 154 (1987).
[2] J. Güémez, S. Velasco, and A. C. Calvo Hernández, Physica A **152**, 226 (1988); A **152**, 243 (1988).
[3] J. S. Rowlinson and G. B. Woods, Physica A **164**, 117 (1990).
[4] B. F. Chmelka, A. V. McCormick, L. C. de Menorval, R. D. Levine, and A. Pines, Phys. Rev. Lett. **66**, 580 (1991).
[5] See, for instance, J. P. Hansen and I. R. McDonald, *Theory of Simple Liquids*, 2nd ed. (Academic Press, London, 1986).
[6] H. Reiss, H. L. Frisch, and J. L. Lebowitz, J. Chem. Phys. **31**, 369 (1959); E. Helfand, H. L. Frisch, and J. L. Lebowitz, *ibid.* **34**, 1037 (1961).
[7] D. Henderson, Mol. Phys. **30**, 971 (1975).
[8] M. Baus and J. L. Colot, Phys. Rev. A **36**, 3912 (1987).
[9] M. Baus and J. L. Colot, J. Phys. C **19**, L643 (1986).